

Quantum Magnetism in Kamchatkan Copper Minerals

Masayoshi Fujihala

Advanced Science Research Center, Japan Atomic Energy Agency, Tokai, Ibaraki 319-1195, Japan

Quantum spin states in low-dimensional magnetic materials have been extensively studied because of emergent spin gaps and topological features. Intensive studies of one-dimensional linear spin chain antiferromagnets have succeeded in capturing several quantum spin states, such as the Tomonaga-Luttinger spin liquid state and the Haldane state. However in many cases, the lack of suitable model materials of theoretical models has hindered the observation of exotic quantum spin states. In the study of low-dimensional quantum magnets, minerals are often employed as model materials. For example, azurite ($\text{Cu}_2(\text{CO}_3)(\text{OH})_2$)¹⁾ and herbertsmithite ($\text{ZnCu}_3(\text{OH})_6\text{Cl}_2$)²⁾ have been identified as candidates for the diamond chain (1D) and kagome lattice (2D) antiferromagnet, and many experimental studies have been performed. In this presentation, I will present results of comprehensive studies of magnetism in Kamchatkan copper minerals fedotovite³⁾ and atlasovite⁴⁾.

Fedotovite $\text{K}_2\text{Cu}_3\text{O}(\text{SO}_4)_3$ is a candidate of new quantum spin systems, in which the edge-shared tetrahedral (EST) spin clusters consisting of Cu^{2+} are connected by weak intercluster couplings forming a one-dimensional array (Fig. 1(a)). Comprehensive experimental studies by magnetic susceptibility, magnetization, heat capacity, and inelastic neutron scattering measurements reveal the presence of an effective $S = 1$ Haldane state below $T \cong 4$ K. Rigorous theoretical studies provide an insight into the magnetic state of $\text{K}_2\text{Cu}_3\text{O}(\text{SO}_4)_3$: an EST cluster makes a triplet in the ground state and a one-dimensional chain of the EST induces a cluster-based Haldane state (Fig 1(b)).

Atlasovite $\text{KCu}_6\text{AlBiO}_4(\text{SO}_4)_5\text{Cl}$ is a first candidate of a square kagome lattice spin-1/2 antiferromagnet (Fig. 2). The μSR measurement shows no long-range ordering down to 58 mK, roughly three orders of magnitude lower than the nearest neighbor interactions. The INS spectrum exhibits a streak-like gapless excitation and flat dispersionless excitation, consistent with powder-averaged spinon excitations. Our experimental results strongly suggest the formation of a gapless QSL in $\text{KCu}_6\text{AlBiO}_4(\text{SO}_4)_5\text{Cl}$ at very low temperature close to the ground state.

I will also discuss why I focused on Kamchatkan copper minerals as candidates for exotic quantum magnets.

Reference

- 1) H. Kikuchi *et al.*, Phys. Rev. Lett. **94** (2005) 227201.
- 2) P. Mendels and F. Bert, J. Phys. Soc. Jpn. **79** (2010) 011001.
- 3) M. Fujihala *et al.*, Phys. Rev. Lett. **120** (2018) 077201.
- 4) M. Fujihala *et al.*, Nat. Commun. **11**, 3429 (2020).

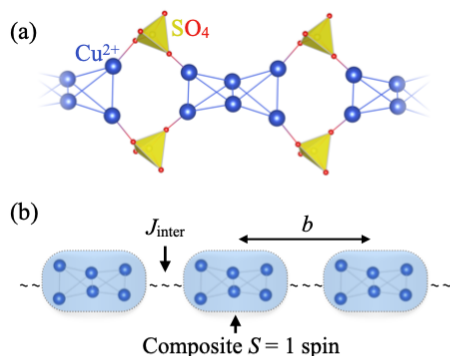


Fig. 1: (a) Crystal structure of $\text{K}_2\text{Cu}_3\text{O}(\text{SO}_4)_3$. The edge-shared tetrahedral spin cluster of the Cu^{2+} ions (blue) displayed with nearby oxygen (red) and sulfur (yellow) ions. (b) Schematic effective model of cluster-based $S = 1$ Haldane chain.

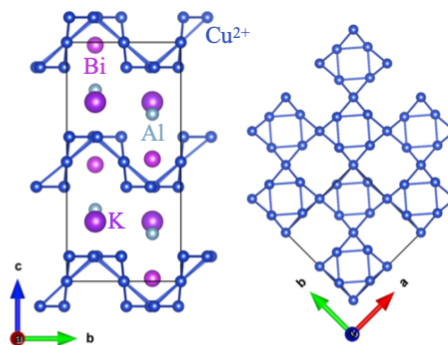


Fig. 2: Crystal structure of $\text{KCu}_6\text{AlBiO}_4(\text{SO}_4)_5\text{Cl}$. The square kagome lattice of the Cu^{2+} ions (blue) displayed with nearby nonmagnetic ions.

Discovery of Magnetocaloric Materials by Machine Learning

Yoshihiko Takano

National Institute for Materials Science (NIMS), Tsukuba 305-0047 Japan

University of Tsukuba, Tsukuba 305-8577 Japan

The liquefaction of hydrogen gas using the magnetocaloric effect (MCE) is expected for the development of hydrogen society to prevent the global warming. The magnitude of the magnetic entropy change (ΔS_M) tends to peak at a material's magnetic ordering temperature, such as Curie temperature, and its maximum value for a ΔH strongly depends on the material itself. Thus, it is highly desired to discover suitable materials showing marked MCE in the working temperature range. However, it still remains challenging to explore and design new materials that can exhibit a remarkable MCE. To tackle this issue, we constructed a machine learning (ML) model for predicting ΔS_M^{MAX} only based on the applied field change and chemical formula of the materials. We used the gradient boosting method as implemented in XGBoost [1] package, and optimized hyperparameters in the ML model using HyperOpt [2], and obtained a best model that gives a mean absolute error of 1.8 (J kg⁻¹ · K⁻¹) for the test dataset and R² = 0.85 as depicted in Fig. 1. Then, we applied this ML model in conjunction with our domain expertise to filter possible candidates for experimental verification. Through this approach, we synthesized the most promising candidate and experimentally found that HoB₂ exhibits ΔS_M^{MAX} of 40 J kg⁻¹ K⁻¹ (0.35 J cm⁻³ K⁻¹) for a field change of 5 T [3], to our knowledge the highest value among all known bulk second-order phase transition solid magnets in this temperature range as shown in Fig. 2. Therefore, the discovered material HoB₂ would be highly suitable for liquefaction of hydrogen gas.

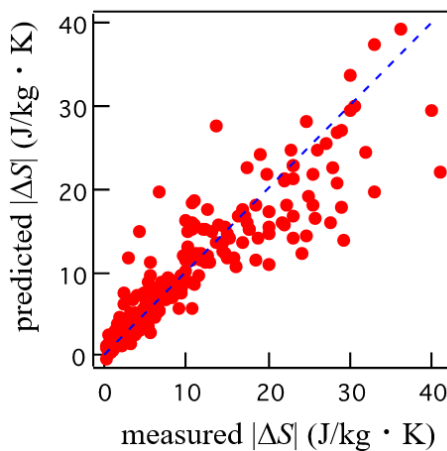


Fig. 1 ML model for prediction of magnetocaloric materials.

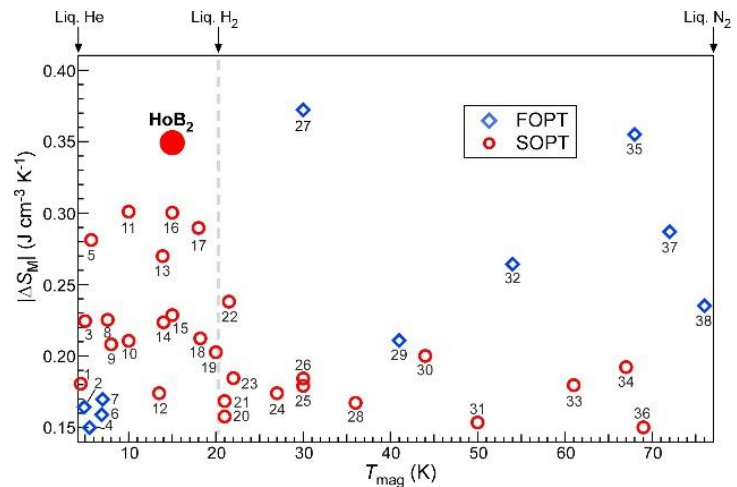


Fig. 2 Comparison of ΔS of HoB₂ with current known magnetocaloric materials between 4.2 to 77 K

Reference

- 1) Reference style T. Chen and C. Guestrin, in proceedings of KDD'16 785 (2016).
- 2) J. Bergstra, B. Komer, C. Eliasmith, D. Yamins, and D. D. Cox, Comput. Sci. Discov. 8, 014008 (2015).
- 3) P. B. Castro, K. Terashima, T. D. Yamamoto, Z. Hou, S. Iwasaki, R. Matsumoto, S. Adachi, Y. Saito, P. Song, H. Takeya, and Y. Takano, NPG Asia Materials 12:35, (2020).

Search for new superconductors

using bulk combinatorial chemistry method

Akira Iyo

National Institute of Advanced Industrial Science and Technology (AIST), Tsukuba 305-8568, Japan

Effective methodologies for developing innovative, high-performance materials are essential for sustaining materials research in Japan, where the human resources are shrinking. We have been testing whether new superconductors (SCs) can be discovered efficiently using the concept of combinatorial chemistry (CC) ¹, which has a successful history in the field of drug discovery. Keys to the success of CC are the simultaneous synthesis of many compounds and high-throughput screening to extract substances with the desired function.

Figure 1 shows the protocol for searching for new SCs by the CC method (called the bulk combinatorial (BC) method because bulk samples are used). A sample consisting of many compounds is prepared by heating a pellet with randomly selected elements for a short period of time (the simultaneous synthesis of many compounds). Because of the huge diamagnetic response associated with the superconducting transition, even a small fraction (~0.01%) of new SCs accidentally formed in the pellet can be detected by a high-sensitive magnetometer (high-throughput screening).

Figure 2 shows the examples of SCs discovered by the BC method ². SCs with various structure types were found. Some SCs would not have been synthesized without the BC method. Unexpected discoveries are another advantage of the BC method. Through this study, we are convinced that the BC method is a very efficient method to find new SCs.

We believe that the BC method can be applied not only to SCs but also to other functional materials. It is then important to find high-throughput screenings suitable for the material's properties. Furthermore, the BC method has the potential to grow into an even more powerful method by combining materials informatics to determine more promising starting elements and sample preparation conditions etc.

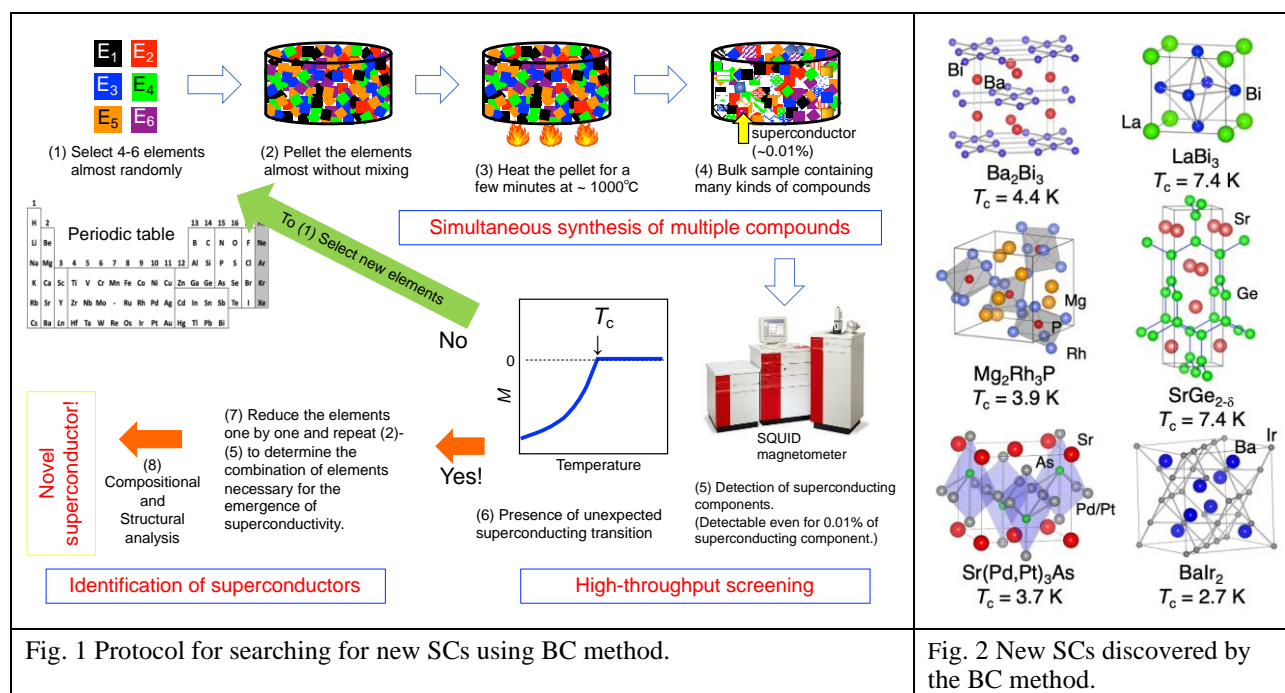


Fig. 1 Protocol for searching for new SCs using BC method.

Fig. 2 New SCs discovered by the BC method.

References

- 1) Materials Informatics –Kaihatsu Jirei Saizensen–, NTS, ISBN978-4-86043-708-4, P255-266
- 2) A. Iyo et al. Phys. Rev. Mater. **3** (2019) 124802. A. Iyo et al, Inorg. Chem. **59** (2020) 12397. etc.

Intercalation compounds of 1D-structured transition metal trichalcogenides

M. Fujioka
(Hokkaido University)

In general, intercalation into two-dimensional (2D) materials is well known to induce lattice expansion. However, in the case of one-dimensional (1D) materials, the effect of intercalation on the structure and physical properties is not understood comprehensively. Transition metal trichalcogenides (TMTs) are typical 1D materials and comprise 1D trigonal prismatic units surrounded by van der Waals gap. This three-dimensionally spread van der Waals gap can accommodate three equivalents or more guest ions, although the capacity of 2D material is only one equivalent in general. Based on such a high ion accommodating capacity, 1D materials are expected to show various functionality. However, the detailed crystal structure of 1D materials after intercalation has not been experimentally revealed because it is challenging to intercalate guest ions into 1D materials while maintaining high crystallinity.

In this study, Ag ions were intercalated into ZrTe_3 , which is a member of the TMT family with a 1D structure, via a proton-driven ion introduction (PDII)(Fig. 1): solid-state intercalation process¹⁾. The change in crystal structure and physical properties according to Ag concentration were clarified for the first in our study. Here, six essential novel findings of TMT intercalation compounds are listed below.

- 1D trigonal prismatic structure in ZrTe_3 changed to 1D octahedral structure via Ag intercalation using PDII. During the structural transition, the long-range order of crystals was disrupted, despite the retention of the 1D order. This unique state was referred to as a “quasi-amorphous phase” in this study.
- The formation of the quasi-amorphous phase affords a reasonable explanation for the previously reported contradiction that the crystal structure did not change in the initial stage of intercalation into TMTs²⁾.
- The quasi amorphous phase shows the homogeneous Ag concentration in the macroscopic region via SEM-EDS measurements but inhomogeneous Ag concentration in the nanoscale region via STEM-EDS measurements. DFT calculations indicated that the origin of the nanoscale Ag inhomogeneity is the attractive interaction between Ag ions.
- In the quasi-amorphous phase, the electric properties changed continuously from superconductivity to semiconductivity according to the Ag concentration. In particular, the highest T_c (6.3 K) and B_{c2} (12 T) were obtained in $\text{Ag}_{0.5}\text{ZrTe}_3$ among TMT intercalation compounds. The nanoscale Ag inhomogeneity explains the enhancement of B_{c2} and the coexistence of both CDW and bulk superconductivity reported so far³⁾.
- Due to the attraction between Ag ions, the activation energy for pair diffusion of Ag ions is much lower than that for single diffusion. The former is less than 0.05 eV along the b -axis. This material should show anisotropic fast Ag ion diffusion.
- Judging the attraction or repulsion between guest ions in TMTs would predict whether to induce a quasi-amorphous phase or simple lattice expansion like 2D materials. A current overview of TMT intercalation compounds was presented based on this interaction between guest ions.

The quasi-amorphous phase with the 1D order is the state of matter based on a novel concept. It has the potential to open a pathway to achieve high functionality, such as fast ion diffusivity for low activation energy, a low thermal conductivity derived from the phonon scattering in a quasi-amorphous state, and high controllability of the electric carrier density based on the high guest-ion accommodation capacity.

Reference

- 1) M. Fujioka, et al., *J. Am. Chem. Soc.*, **139**, 17987 (2017).
- 2) C. Mirri, et al., *Phys. Rev. B*, **89** 035144 (2014).
- 3) X. Zhu, et al., *Phys. Rev. Lett.*, **106**, 246404 (2011).

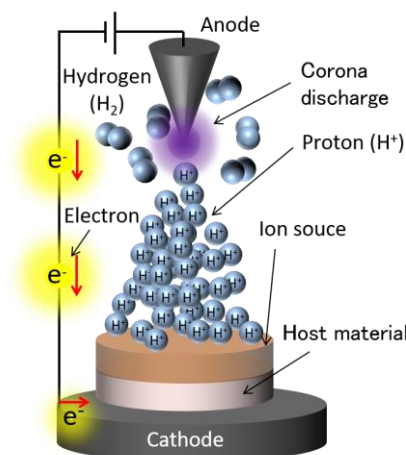


Figure 1. Schematic of PDII.

Layered ruthenium and iridium oxyfluoride thin films fabricated via topochemical fluorination

A. Chikamatsu¹ and T. Hasegawa²

¹Department of Chemistry, Faculty of Science, Ochanomizu University, Tokyo 112-8610, Japan

²Department of Chemistry, The University of Tokyo, Tokyo 113-0033, Japan

Layered ruthenium and iridium oxyfluorides have various crystal structures and oxidation states and exhibit unique physical properties. We fabricated phase-pure and single-crystalline thin films of $\text{Sr}_2\text{RuO}_3\text{F}_2$, $\text{Ca}_2\text{RuO}_{2.5}\text{F}_2$, and $\text{Sr}_2\text{IrO}_{2.5}\text{F}_3$ via topochemical fluorination of Sr_2RuO_4 , Ca_2RuO_4 , and Sr_2IrO_4 using polyvinylidene fluoride and investigated their structures, electronic states, and electron transport properties [1-4]. All the fluorinated films exhibited a largely expanded c -axis than the precursors, indicating that fluorine ions are preferentially inserted into the SrO or CaO rocksalt blocks in the perovskite structures and that the oxygen atoms in the precursor oxides were partially removed upon fluorination. The X-ray photoemission spectroscopy, transmission electron microscope, and density functional theory revealed that $\text{Sr}_2\text{RuO}_3\text{F}_2$ is a Mott insulator with Ru^{4+} states and has two inequivalent F^- sites in the SrO layers [1,2]. On the other hand, $\text{Ca}_2\text{RuO}_{2.5}\text{F}_2$ thin films had the Ru^{3+} state and only one F^- site in the CaO rock-salt blocks [3]. This discrepancy is probably due to the larger lattice distortion in the Ca_2RuO_4 precursor than Sr_2RuO_4 . Both $\text{Sr}_2\text{RuO}_3\text{F}_2$ and $\text{Ca}_2\text{RuO}_{2.5}\text{F}_2$ films were insulating, with resistivity (ρ) of $4.1 \times 10 \text{ } \Omega \text{ cm}$ and $8.6 \times 10^{-2} \text{ } \Omega \text{ cm}$ at 300 K, respectively [1,3]. Moreover, the temperature behavior of ρ of $\text{Ca}_2\text{RuO}_{2.5}\text{F}_2$ thin film was well described by the two-dimensional variable range hopping model [3]. Optical and photoemission measurements of $\text{Sr}_2\text{IrO}_{2.5}\text{F}_3$ thin films revealed that the effective total angular momentum $J_{\text{eff}} = 3/2$ is stabilized upon fluorination owing to the large electronegativity of fluorine [4]. The $\text{Sr}_2\text{IrO}_{2.5}\text{F}_3$ film exhibited a semiconducting behavior described by Efros-Shklovskii variable-range hopping [4]. These results will be useful for modifying electronic states by anion doping to explore unprecedented physical properties in Ruddlesden-Popper-type oxides.

Reference

- 1) K. Kawahara, A. Chikamatsu, T. Katayama, T. Onozuka, D. Ogawa, K. Morikawa, E. Ikenaga, Y. Hirose, I. Harayama, D. Sekiba, T. Fukumura, and T. Hasegawa, *CrystEngComm* **19**, (2017) 313.
- 2) A. Chikamatsu, Y. Kurauchi, K. Kawahara, T. Onozuka, M. Minohara, H. Kumigashira, E. Ikenaga, and T. Hasegawa, *Phys. Rev. B* **97**, (2018) 235101.
- 3) S. Fukuma, A. Chikamatsu, T. Katayama, T. Maruyama, K. Yanagisawa, K. Kimoto, M. Kitamura, K. Horiba, H. Kumigashira, Y. Hirose, and T. Hasegawa, *Phys. Rev. Mater.* **6**, (2022) 035002.
- 4) T. Maruyama, A. Chikamatsu, T. Katayama, K. Kuramochi, H. Ogino, M. Kitamura, K. Horiba, H. Kumigashira, and T. Hasegawa, *J. Mater. Chem. C* **8**, (2020) 8268.

Expectation to Magnetic of Electrical Motor, Power Electronics in Electrical Vehicle

Keisuke Fujisaki
(Toyota Technological Institute)

Commercial use of electrical vehicle is now expanded year by year for the reduction of environmental impact ¹⁾. The electrical vehicle is driven by electrical motor drive system with an electrical motor and a power electronics technology ²⁾. The electrical motor is driven by magnetic force ³⁾. So the soft magnetic material is used as a motor core to obtain high magnetic flux density, and the hard magnetic material is used as magnetic field of the rotor ⁴⁾.

NO (Non-oriented) silicon steel is mainly used as motor core due to good cost performance. However, to reduce the iron loss, lower iron loss material is commercially used as GO (Grain-oriented) steel, amorphous material and nano-crystal steel. They have a good magnetic performance as low iron loss and high magnetic permeability. When they are applied to the motor core and tribally manufactured, core loss reduction is measured ⁵⁻⁷⁾. Cost reduction is one of the main problems to be realized.

When the inverter excites the magnetic material for the motor drive system, the iron loss usually increases due to the carrier frequency and modulation index characteristics ⁸⁾. Ringing phenomena is observed in GaN-FET inverter excitation because high rising up voltage of fast switching operation makes a resonance with the load. So the ringing iron loss increases in high carrier frequency operation ⁹⁾.

The power electronics circuit needs an inductor with soft magnetic material. So the magnetic material for high frequency operation is now a bottleneck technology to realize the power electronics realization

About 30 years old or so, high frequency magnetic material technology was more advanced than power electronics technology ¹⁰⁾. More than 1 MHz magnetic material and the device were researched and trail manufactured, though high frequency power device such as MOS-FET was under developing. However, since high frequency devices such as IGBT or GaN, SiC devices are researched and in practical use, air core is used as an inductor device or low frequency operation is used.

Ferrite is expected to be for high frequency, but it has small magnetic saturation or is weak for high temperature such as 100 degree or so. Metal powder with magnetization characteristics is developed, but it has small magnetic permeability due to demagnetization characteristics. Magnetic metal sheet with small thickness is expected due to high magnetic permeability. High density of power semiconductor and control one is advances now, so most of the components of the power electronics circuit are often shown to be the magnetic material ⁵⁾.

Magnetics are important technology for the realization of power electronics society and EV society.

Reference

- 1) https://www.jsae.or.jp/roadmap/pdf/tec_02-1.pdf (R04.06.05)
- 2) K. Fujisaki, "Magnetics of Motor Drive System for Electrical Vehicle." IEEE Intermag conf 2021. (2021.4.26-30).
- 3) W. K. H. Panofsky, M. Phillips, "Classical electricity and magnetism, second edition", Addison-Wesley publishing company, 1978.
- 4) Editor: Keisuke Fujisaki, "Magnetic Material for Motor Drive System", Springer-Nature, 2019.12.
- 5) N. Denis, S. Takeda, K. Fujitani, K. Fujisaki, S. Odawara, "Anisotropic Magnetic ore for the Iron Loss Reduction of Permanent Magnet Synchronous Motor," J. Magn. Soc. Japan, Vol. 42, No. 3, pp. 62-71, 2018.5.
- 6) A. Yao, T. Sugimoto, S. Odawara, and K. Fujisaki, "Core losses of a permanent magnet synchronous motor with an amorphous stator core under inverter and sinusoidal excitations," AIP (American Institute of Physics)Advances 8, 056804 (2018).
- 7) N. Denis, M. Inoue, K. Fujisaki, H. Itabashi, T. Yano, "Iron Loss Reduction of Permanent Magnet Synchronous Motor by Use of Stator Core Made of Nanocrystalline Magnetic Material," IEEE Transactions on Magnetics, Volume: 53, Issue: 11, 8110006, 2017, DOI: 10.1109/TMAG.2017.2700471
- 8) K. Fujisaki, R. Yamada, T. Kusakabe, "Difference in Iron Loss and Magnetic Characteristics for Magnetic Excitation by PWM Inverter and Linear Amplifier," IEEEJ-D, Vol. 133, No. 1, pp. 69-76, 2013.
- 9) Haruo Naitoh, Takaya Sugimoto, Fujisaki Keisuke, "Iron loss characteristics of motors fed by fast switching GaN-FET inverters", Electrical Engineering in Japan 214(1), June 2021.
- 10) 白江 公輔, 荒井 賢一, 島田 寛「マイクロ磁気デバイスのすべて—半導体デバイスへの新たななる挑戦」K Books series, 工業調査会, 1992.10.

Magnetic domain structure and magnetic properties of soft magnetic materials

M. Takezawa

Faculty of Engineering, Kyushu Institute of Technology, Kitakyushu 804-8550, Japan

Low-loss soft magnetic materials are used for transformers and motors as magnetic core materials. Because the higher the operational frequency enables miniaturization of the devices, recently, it has become necessary to reduce the loss of soft magnetic materials at high frequencies. For this reason, various soft magnetic materials have been proposed, including amorphous and nanocrystalline materials and molded cores using their magnetic powders¹⁾⁻⁵⁾.

The magnetic properties of these magnetic materials largely depend on the magnetic domain structure⁶⁾⁻⁸⁾. Therefore, it is important to observe the magnetic domain structure of magnetic materials to improve the performance of magnetic materials and devices. We have observed magnetic domains of various soft magnetic materials using magnetic Kerr effect microscopy⁹⁾⁻¹²⁾. In this paper, we report on the relationship between magnetic domain structure and magnetic properties of soft magnetic materials.

Figure 1 shows an example of magnetic domain observation of an oriented Si-Fe sheet used for a transformer. The dark and bright domains in this figure have magnetizations pointing upward and downward, respectively. Fig. 1(a) shows a stripe-shaped magnetic domain pattern parallel to the rolling direction. A motion of 180° domain walls was observed when a magnetic field along the rolling direction was applied. On the other hand, Fig. 1(b) shows the magnetic domain configuration of a Si-Fe sheet with a $50\ \mu\text{m} \times 50\ \mu\text{m}$ square scratch on the sheet surface. It can be seen that magnetic wall motion was pinned at the edge of the scratch, as shown in the figure. It was found through the result that scratches on the surface of the magnetic material suppress magnetic wall motion and cause increased iron losses.

In order to reduce eddy current losses in soft magnetic materials at high frequencies, decreasing the thickness of the sheet is useful. However, it is known that the ratio of the measured value to the classical theoretical value of eddy current loss increases when the sheet thickness decreases below 0.20 mm in non-oriented electrical steel sheets due to changes in the magnetic domain structure¹³⁾. Figure 2 shows the domain structure of 0.35- and 0.15-mm-thick non-oriented Si-Fe sheet at a remanent state. Chemical etching was used for thinning the sheet from the underside to observe the same spot before and after thinning. Stripe domain configuration running parallel to the rolling direction was observed at the thick sheet of 0.35 mm. It was observed that the domain pattern changed to the stripe domain configuration along the transverse direction when the sheet thickness decreased to 0.15 mm, as shown in Fig. 2(b). The stripe domain observed at a small thickness of 0.15 mm is part of the closure domain structure created by the normal magnetization component to the surface. When the magnetization component inclines from the normal direction, the in-plane magnetic field causes the wall motion inside the sheet, which causes a large eddy current loss.

Figure 3 shows the magnetic domain configuration for 6.5% Si-Fe powders. Figs. 3(b) and 3(c) show enlarged images of a part of Fig. 3(a). Pinning of the magnetic wall occurred in the area circled in red, as shown in Fig. 3(b). When the applied magnetic field was increased, the magnetic wall moved, and depinning occurred, as shown in Fig. 3(c). The composition was examined at the locations of the pinning sites by SEM-EDX. At the pinning sites, Mn and S were detected in addition

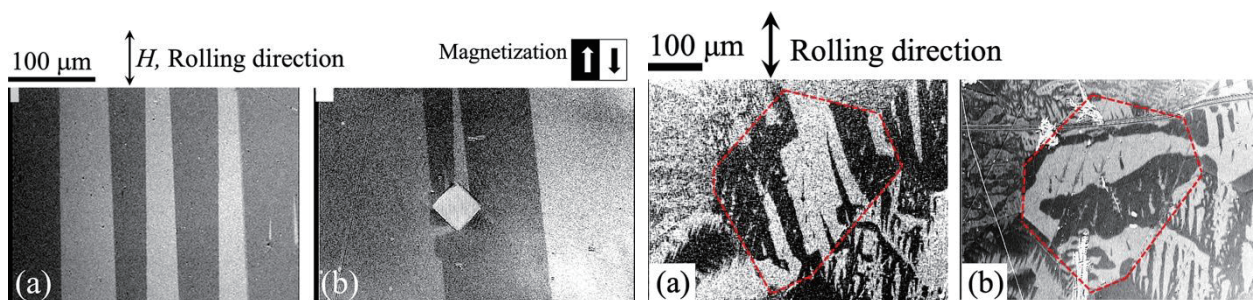


Fig. 1 Magnetic domains of an oriented Si-Fe electrical sheet.

Fig. 2 Magnetic domains of a non-oriented Si-Fe electrical sheet.

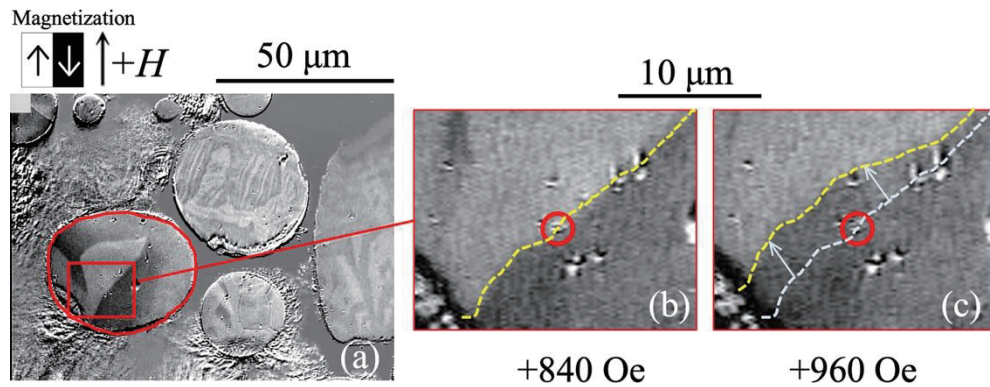


Fig. 3 Magnetic domains of 6.5% Si-Fe powders.

to Fe and Si. It was found that Mn-S included in the magnetic powder causes pinning of the magnetic domain wall. In concluding, we have described that scratches, impurities, and changes in sheet thickness affect the magnetic domain structure of soft magnetic materials and cause an increase in their iron loss. In the future, it is expected that magnetic domain observation of various soft magnetic materials, such as nanocrystalline materials, will be further developed to achieve higher efficiency and lower loss in electric devices.

Reference

- 1) K. Takenaka, A.D. Setyawan, Y. Zhang, P. Sharma, N. Nishiyama, and A. Makino, *Mater. Trans.*, **56**, 372 (2015).
- 2) M. Ohta, Y. Yoshizawa, M. Takezawa, and J. Yamasaki, *IEEE Trans. Magn.*, **46**, 203 (2010).
- 3) Y. Yoshizawa, S. Fujii, D.H. Ping, M. Ohnuma, and K. Hono, *Mater. Sci. Eng.*, **375**, 207 (2004).
- 4) W. Qin, F. Xu, Y.J. Wu, W.L. Gao, J.C. Tang, Y.W. Du, and Y.F. Zhang, *Phys. Stat. Sol.*, **202**, 476 (2005).
- 5) T. Nonaka, S. Zeze, S. Makino, M. Ohto, *IEEJ Trans. IA*, **139**, 873 (2019).
- 6) M. Fujikura, H. Murakami, Y. Ushigami, S. Arai, and K. Iwata, *IEEE Trans. Magn.*, **51**, #2001604 (2015).
- 7) J. Yamasaki, M. Takajo, and F.B. Humphrey, *IEEE Trans. Magn.*, **29**, 2545 (1993).
- 8) R.D. Gomez, T.V. Luu, A.O. Pak, K.J. Kirk, and J.N. Chapman, *J. Appl. Phys.*, **85**, 6163 (1999).
- 9) M. Takezawa, J. Yamasaki, T. Honda, and C. Kaido, *J. Magn. Magn. Mater.*, **254–255**, 167 (2003).
- 10) M. Takezawa, K. Kitajima, Y. Morimoto, J. Yamasaki, and C. Kaido, *IEEE Trans. Magn.*, **42**, 2790 (2006).
- 11) H. Miyata, Y. Morimoto, and M. Takezawa, *J. Magn. Soc. Jpn.*, **38**, 169 (2014).
- 12) Z. Lei, T. Horiuchi, I. Sasaki, C. Kaido, M. Takezawa, S. Hata, Y. Horibe, T. Ogawa, and H. Era, *J. Mag. Soc. Jpn.*, **40**, 8 (2016).
- 13) C. Kaido and T. Wakisaka, *IEEJ Trans. FM*, **117**, 685 (1997).

Basics of Power Electronics

Nobukazu Hoshi
(Tokyo University of Science)

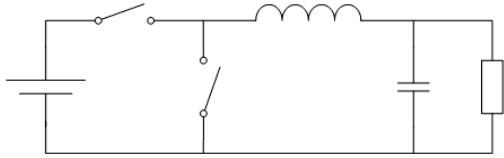
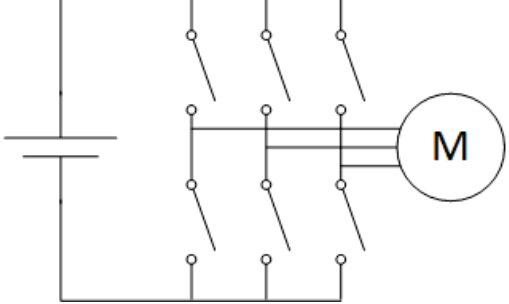
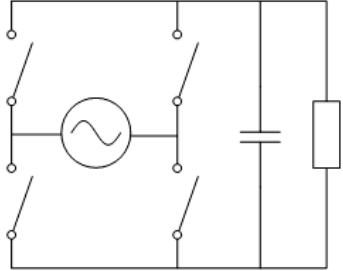
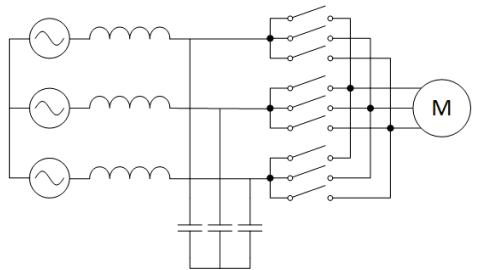
Power electronics is a technology that integrates mainly three fields which are devices, circuits, and control technologies. In power electronics technology, input power is converted to the output power form, which is expected by the load, by turning semiconductor switches on and off. The size, voltage, and capacity of power electronic applications are wide-ranging from large devices such as high voltage DC power transmission and frequency converters to small devices such as point-of-load (POL) converters mounted on a motherboard in a personal computer. The basic principle remains the same in any application, and power conversion is performed by turning the semiconductor switch on and off. Table 1 shows the types of power conversion circuits and typical examples of each circuit. Although the switch is schematically drawn in the figure, diodes, IGBTs (insulated gate bipolar transistors), and MOSFETs (metal-oxide-semiconductor field-effect transistors) are used in single or in combination.

The desired output is obtained in each circuit by controlling the switching period, duty ratio, and phase of switches. In addition, the switching period tends to be shorter, i.e., the switching frequency tends to be higher to reduce the size of the device and improve the quality of the output waveform.

Reference

- 1) Kawamura, et.al, "Introduction to Power Electronics (Revised Edition)", Corona Publishing Co. Ltd., (2022).

Table 1: Types of power conversion circuits and their typical examples.

Input / Output	DC	AC
DC	<p>DC/DC converter, chopper</p>  <p>Buck converter</p>	<p>Inverter</p>  <p>Three-phase inverter</p>
AC	<p>Rectifier</p>  <p>Capacitor input rectifier</p>	<p>Matrix converter</p>  <p>Three-phase to three-phase matrix converter</p>

Magnetic properties expected of soft magnetic materials by motor designers

M. Hazeyama

(Advanced Technology R&D Center, Mitsubishi Electric Corporation, Amagasaki 661-8661, Japan)

Against the background of acceleration of worldwide decarbonization, it is predicted that there will be an acceleration of electrification, mainly in the automobile and aircraft fields in the future[1], and motors are attracting attention as a key part of this electrification. On the other hand, in terms of electric power demand across all industries in Japan, motors currently account for half of the total demand [2].

There are two main types of motors: induction motors(IM) and permanent magnet(PM) motors. The former is mainly driven at commercial frequencies (50 Hz and 60 Hz), while the latter is mainly driven by inverters capable of variable speed driving, and this is attracting attention as a motor for electrification. Therefore, it is necessary to consider the efficiency improvements in the motor based on the type and driving method of the motor. Therefore, in this lecture, we summarize the causes of motor loss according to the type of motor and the driving method and describe expectations for soft magnetic materials for each of the motor types.

Firstly, a schematic diagram of the loss breakdown of a commercial frequency-driven IM and an inverter-driven PM motor is shown in Figure 1. Figure 1 demonstrates the percentage of the total loss at 100%. In the induction machine, primary copper loss mainly occurs in the stator conductor and secondary copper loss mainly occurs in the rotor conductor. In addition, the harmonic component of iron loss is also relatively high in inverter drives. Therefore, a different approach is required to improve the efficiency of each motor. Figure 2 shows the relationship between the magnetic properties of each motor (B_{50}) and the iron loss ($W_{10}/400$). The overall demand for soft magnetic materials is high magnetic flux density and low iron loss.. However, as copper loss is the main cause of loss in commercial induction machines, the motor current can be reduced by increasing the magnetic flux density. In the case of permanent magnet motors for electrification, however, this is mainly iron loss, so materials that reduce iron loss are required.

Reference

- 1) J.Inst.Elect.Engnr.Jpn Vol.142, No.5, pp.284-287, 2022(Japanese)
- 2) Nikkei Electronics, Vol.1055, pp.34-41, 2011(Japanese)

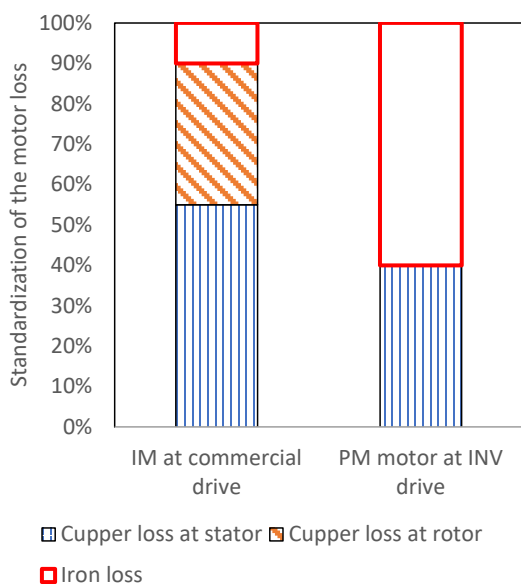


Fig.1 Loss breakdown of a commercial frequency-driven IM and an inverter-driven PM motor

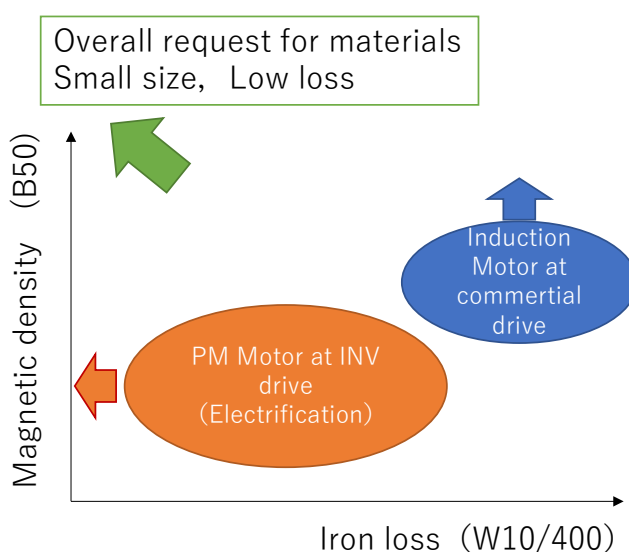


Fig.2 Relationship between magnetic properties of each motor

Recent trend in soft magnetic material for power electronics

I. Nakahata¹, K. Mori² and H. Matsumoto¹

¹ Materials Research Center, TDK Corporation, Narita 286-8588, Japan

² Magnetics business group, TDK Corporation, Narita 286-8588, Japan

Magnetic materials are roughly classified into both metallic magnetic materials and oxide magnetic materials by their composition. In addition, magnetic materials are also classified into both soft magnetic materials showing the smaller coercive force (H_c) and hard magnetic materials showing the large H_c in their magnetic properties.

Ferrite materials are well known as typical oxide magnetic materials. Since OP magnet and CuZn ferrite core were invented by Kato and Takei in 1930's, various kinds of hard/soft ferrites have been developed and used in many applications.

Generally, as shown in Fig. 1, ferrite materials show the low saturation magnetic flux density compared to the silicon steel such as metallic soft magnetic materials. However, ferrite materials with a higher electrical resistivity exhibit the excellent magnetic characteristics in high frequency. From the above reason, soft ferrites have been widely used as the core of inductor and transformer for high frequency application, and new materials are continuously being developed to contribute for the advancement of the power electronics.

MnZn ferrites and NiCuZn ferrites are known as representative materials of soft ferrite.

However, suitable applications are different because these ferrites show different magnetic characteristics. For example, as shown in figure 2, appropriate operating frequency range for each ferrite is differed by their permeability range. In addition, even for only MnZn ferrite, there are various materials with different features such as the temperature dependency and the high frequency characteristic. Therefore, it is important to choose suitable materials for applications considering magnetic characteristics of each magnetic materials.

On the other hand, power electronics have been required to handle increasingly large power with small volume in recent years. Thereby, metallic soft magnetic materials with a high saturation magnetic flux density are attracting attention, and the material development of that is being actively advanced.

In the presentation, recent topics of the development of ferrite materials and metallic soft magnetic materials for power electronics will be reported.

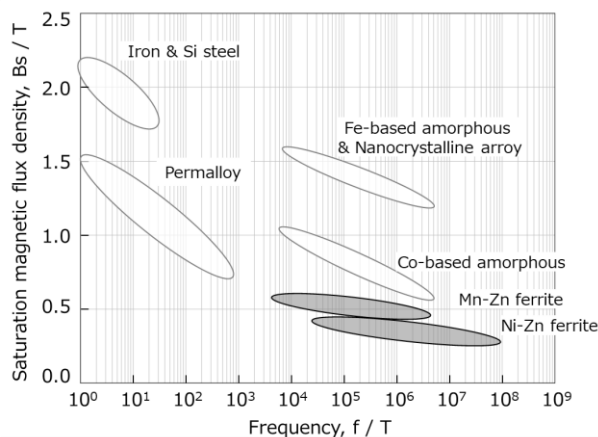


Figure 1. The saturation magnetic flux density and appropriate frequency range for representative soft magnetic materials

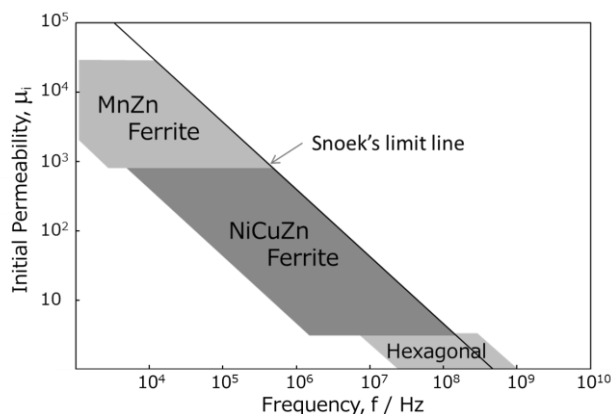


Figure 2. Schematic image of relationship between initial permeability range of ferrites and its appropriate operating frequency range.¹⁾

Reference

- 1) T. Hiraga: Ferrite (in Japanese), p.89 (Maruzen, Tokyo,1986)